Supplementary

Effects of crystal phase and composition on structurally ordered Pt-Co-Ni/C ternary intermetallic electrocatalysts for formic acid oxidation reaction

Lingxuan Chen[a], Jing Zhu[a], Cuijuan Xuan[a], Weiping Xiao[a], Kedong Xia[a], Weiwei Xia[b, c], Chenglong Lai[a], Huolin L. Xin[b], Deli Wang[a]*

[a.] *Key laboratory of Material Chemistry for Energy Conversion and Storage (Huazhong University of Science and Technology), Ministry of Education, Hubei Key Laboratory of Material Chemistry and Service Failure, School of Chemistry and Chemical Engineering, Huazhong University of Science and Technology, Wuhan 430074, PR China*

**Email: wangdl81125@hust.edu.cn.*

[b.] *Center for Functional Nanomaterials, Brookhaven National Laboratory, Upton, NY 11973, USA*

[c.] *SEU-FEI Nano-Pico Center, Key Laboratory of MEMS of the Ministry of Education, Southeast University, Nanjing 210096, China*

Table S1. XRD Results of $PtCo_xNi_{1-x}/C$ annealing at 700 °C for 2 h.

	Structure	Lattice parameter a / nm	Lattice parameter c / nm	Domain size /nm
PtCo	Tetragonal	0.3799	0.3700	6.0
$PtCo_{0.75}Ni_{0.25}$	Tetragonal	0.3802	0.3673	6.6
$PtCo_{0.5}Ni_{0.5}$	Tetragonal	0.3820	0.3657	7.4
$PtCo_{0.25}Ni_{0.75}$	Tetragonal	0.3812	0.3631	
	Cubic	0.3737	-	
PtNi	Cubic	0.3735	-	10

Table S2. Comparison of activity (peak-current density in the anodic sweep) for various FAOR catalysts from literatures.

Catalysts	Activity	Activity of reference	Electrolyte	Refs
$Pt_1Au_1Ru_1$	1.044 A mg_{Pt}^{-1}	0.254 A mg_{Pt}^{-1}	0.5 M H_2SO_4 + 0.5 M HCOOH	1
Pt-CeO_2/RGO/CCE	60 mA cm^{-2}	6.6 mA cm^{-2}	0.1 M H_2SO_4 + 0.1 M HCOOH	2
Pt-Ni/CCE	1.82 mA cm^{-2}	0.31 mA cm^{-2}	0.1 M H_2SO_4 + 0.5 M HCOOH	3
PdNPs/NCB/CCE	24.9 mA cm^{-2}	10.78 mA cm^{-2}	0.5 M H_2SO_4 + 0.5 M HCOOH	4
Pt-Sn/CCE	1.3 mA cm^{-2}	0.08 mA cm^{-2}	0.5 M H_2SO_4 + 0.5 M HCOOH	5
AuPt@Pd/C	0.83 A mg_{Metal}^{-1}	0.52 A mg_{Metal}^{-1}	0.5 M H_2SO_4 + 0.5 M HCOOH	6
PtAu	0.80 A mg_{Metal}^{-1}	-	0.5 M H_2SO_4 + 0.5 M HCOOH	7
$Fe_{43}Pt_{37}Au_{20}$	2.81 A mg_{Pt}^{-1}	-	0.5 M H_2SO_4 + 0.5 M HCOOH	8
Pt/RGO/CC	0.12 A mg_{Pt}^{-1}	-	0.5 M H_2SO_4 + 0.5 M HCOOH	9
$Pt_1@Pd_{75}/C$	2.3 A mg_{Metal}^{-1}	1.0 A mg_{Pd}^{-1}	0.5 M H_2SO_4 + 0.5 M HCOOH	10
Pt-MoS_2/RGO	6.8 mA cm^{-2}	1.4 mA cm^{-2}	0.5 M H_2SO_4 + 0.5 M HCOOH	11
CuFePt/RGO	0.48 A mg_{Pt}^{-1}	0.09A mg_{Pt}^{-1}	0.5 M H_2SO_4 + 0.5 M HCOOH	12
PtPd	1.29 A mg_{Metal}^{-1}	0.45 A mg_{Pt}^{-1}	0.5 M H_2SO_4 + 0.5 M HCOOH	13
Pt_3Zn_7/C	1.46 A mg_{Pt}^{-1}	0.563 A mg_{Pt}^{-1}	0.5 M H_2SO_4 + 0.5 M HCOOH	14
Pt_2CoNi/C	2.16 A mg_{Pt}^{-1}	0.956 A mg_{Pt}^{-1}	0.5 M H_2SO_4 + 0.5 M HCOOH	This work

Table S3. Average atomic ratios of Co/Pt and Ni/Pt for $PtCo_xNi_{1-x}$/C after CA measurements.

Catalyst			Average ratios	Retention (%)
PtCo	Co/Pt	Initial	1	
		10 Ks	0.351	35.1
$PtCo_{0.75}Ni_{0.25}$	Co/Pt	Initial	0.75	
		10 Ks	0.636	84.8
	Ni/Pt	Initial	0.25	
		10 Ks	0.182	72.8
$PtCo_{0.5}Ni_{0.5}$	Co/Pt	Initial	0.5	
		10 Ks	0.429	85.8
	Ni/Pt	Initial	0.5	
		10 Ks	0.357	71.4
$PtCo_{0.25}Ni_{0.75}$	Co/Pt	Initial	0.25	
		10 Ks	0.203	81.2
	Ni/Pt	Initial	0.75	
		10 Ks	0.492	65.6
PtNi	Ni/Pt	Initial	1	
		10 Ks	0.818	81.8

Table S4. XRD Results of $PtCo_{0.5}Ni_{0.5}$/C annealing at different temperatures

	Structure	Lattice parameter a / nm	Lattice parameter c / nm	Domain size /nm	$I_{(100)}/I_{(101)}$ (%)
Pt	Cubic	0.3923			
$PtCo_{0.5}Ni_{0.5}$-500	Cubic	0.3747		5.1	
$PtCo_{0.5}Ni_{0.5}$-600	Tetragonal	0.3819	0.3672	6.2	11.38
$PtCo_{0.5}Ni_{0.5}$-700	Tetragonal	0.3820	0.3657	7.4	14.05

Table S5. Average ratios of Co/Pt and Ni/Pt of $PtCo_{0.5}Ni_{0.5}$/C annealing at different temperatures for 2 h after CA measurements.

Catalyst			Average ratios	Retention (%)
$PtNi_{0.5}Co_{0.5}$-500	Co/Pt	Initial	0.5	
		10 Ks	0.328	65.6%
	Ni/Pt	Initial	0.5	
		10 Ks	0.311	62.2%
$PtNi_{0.5}Co_{0.5}$-600	Co/Pt	Initial	0.5	
		10 Ks	0.379	75.8%
	Ni/Pt	Initial	0.5	
		10 Ks	0.345	69.0%
$PtNi_{0.5}Co_{0.5}$-700	Co/Pt	Initial	0.5	
		10 Ks	0.429	85.8%
	Ni/Pt	Initial	0.5	
		10 Ks	0.357	71.4%

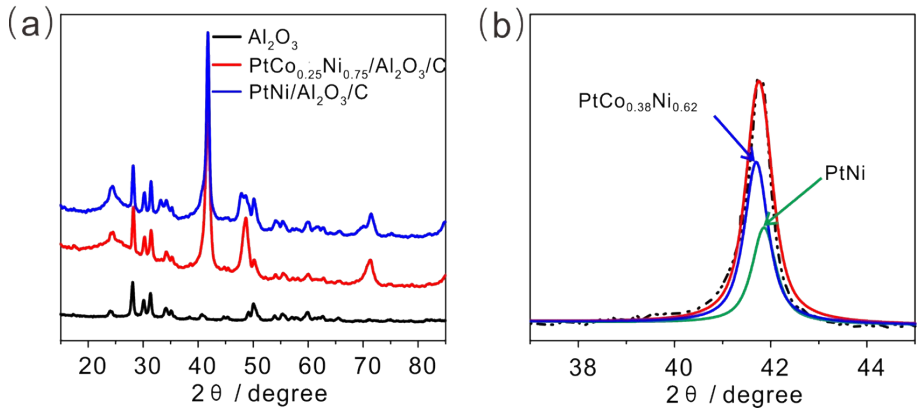

Figure S1. (a) XRD patterns for $PtCo_{0.25}Ni_{0.75}/Al_2O_3/C$ and $PtNi/Al_2O_3/C$; **(b)** (111) plane of PtNi alloy and PtCo intermetallic phase of $PtCo_{0.25}Ni_{0.75}/C$ NCs. Peaks fitting are based on identical domain size, namely the almost same half-peak breadth.

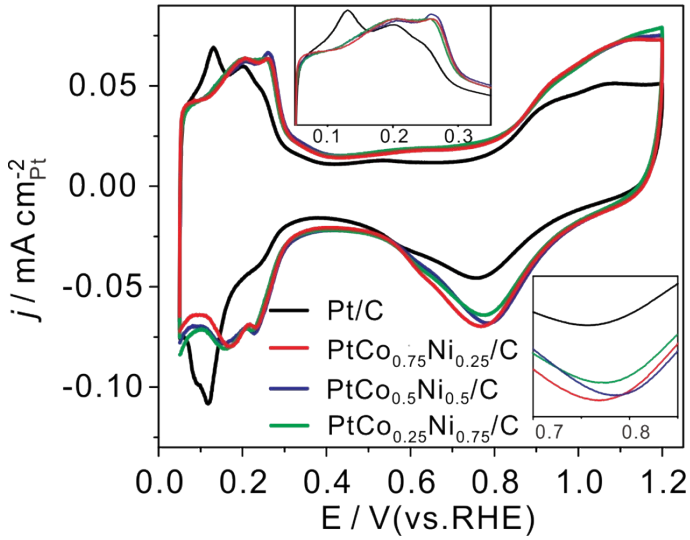

Figure S2. CV in 0.5 M H_2SO_4 purged with N_2 at room temperature and a sweep rate of 50 mV s^{-1}.

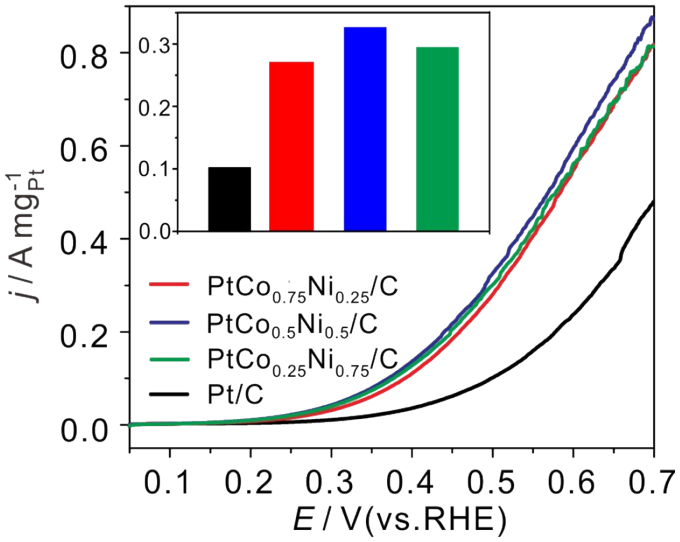

Figure S3. LSV in 0.5 M H_2SO_4 + 0.5 M HCOOH at a sweep rate of 1 mV s^{-1}.

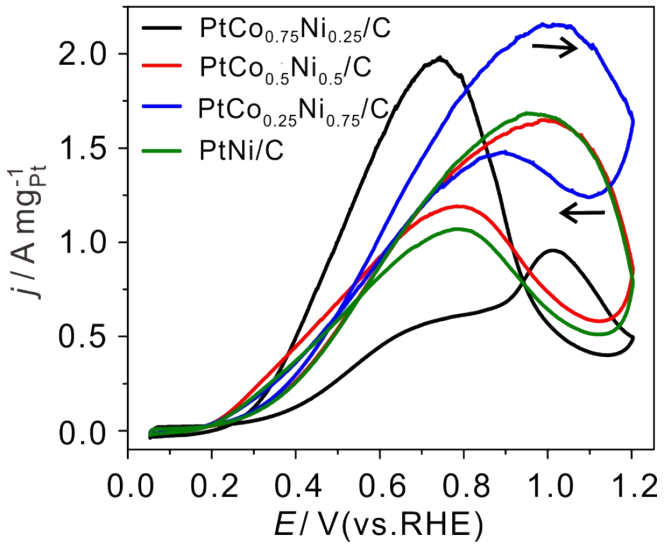

Figure S4. CV in 0.5 M H_2SO_4 + 0.5 M HCOOH purged with N_2, sweep rate of 50 mV s^{-1}, at room temperature.

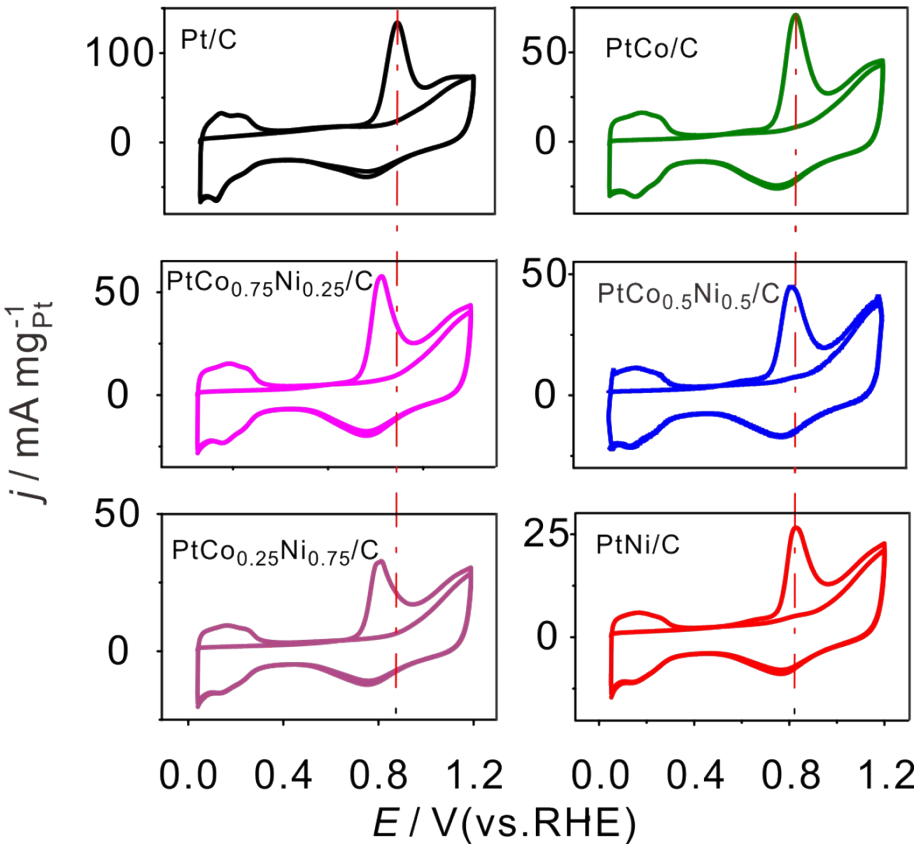

Figure S5. CO stripping voltammograms curves of $PtCo_xNi_{1-x}/C$ annealing at 700 °C for 2 h and Pt/C catalysts in 0.5 M H_2SO_4 solution at room temperature and at a scan rate of 50 mV s^{-1}.

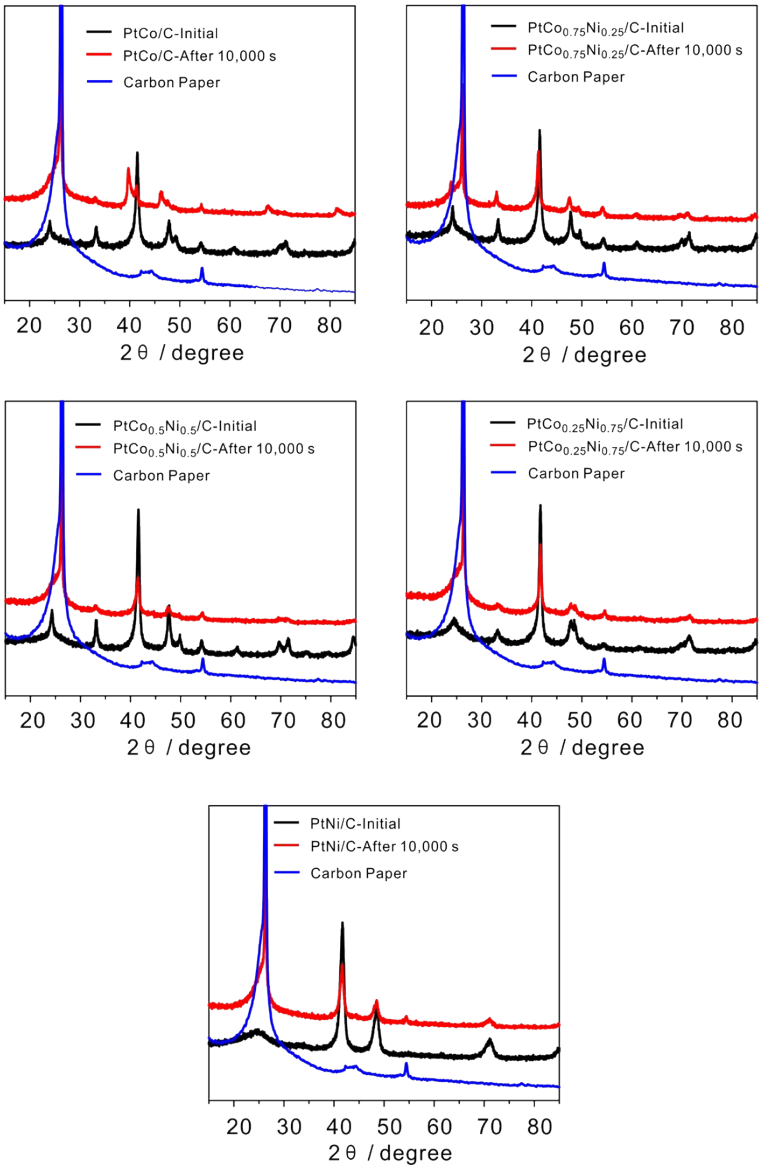

Figure S6. XRD patterns for $PtCo_xNi_{1-x}/C$ annealing at 700 °C for 2 h before and after **CA** measurements.

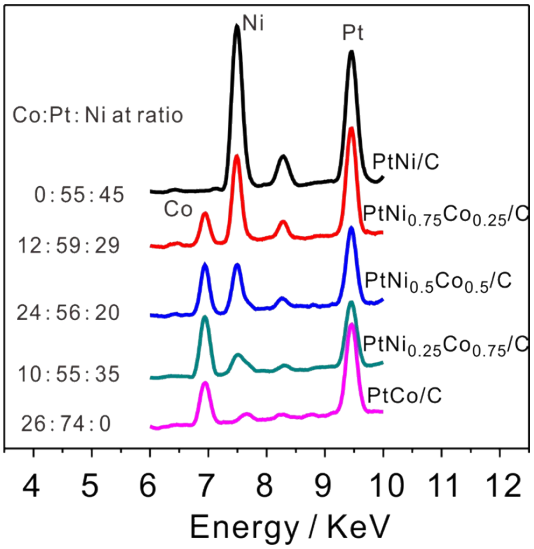

Figure S7. XRF patterns of $PtCo_xNi_{1-x}/C$ after CA measurements.

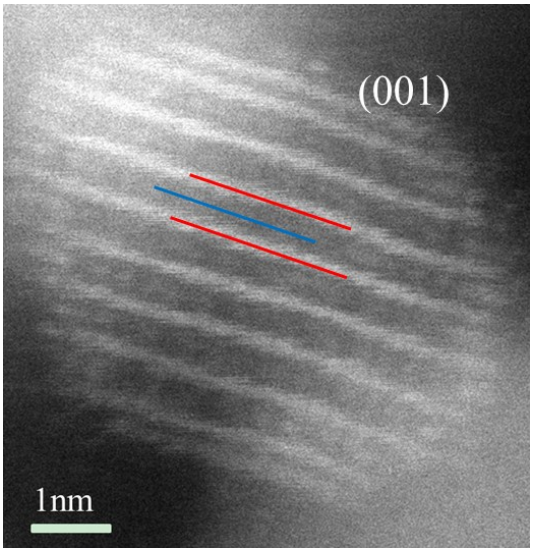

Figure S8. HRTEM micrographs of an individual particle of $PtNi_{0.5}Co_{0.5}/C$ after CA measurements.

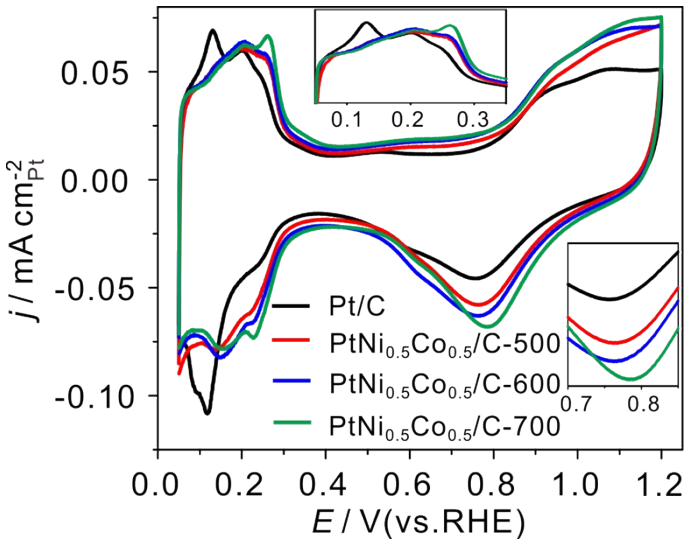

Figure S9. CV in 0.5 M H_2SO_4 purged with N_2 at room temperature and a sweep rate of 50 mV s^{-1}. The inset shows enlarged region of hydrogen region and oxygen region.

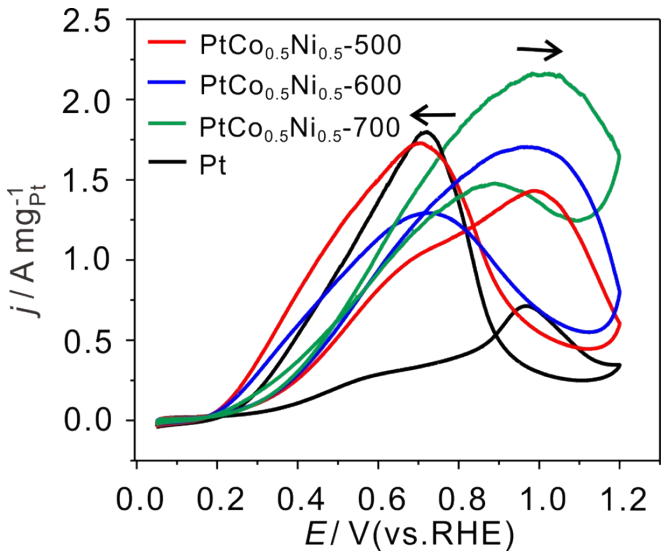

Figure S10. CV in 0.5 M H_2SO_4 + 0.5 M HCOOH purged with N_2, sweep rate of 50 mV s^{-1}, at room temperature.

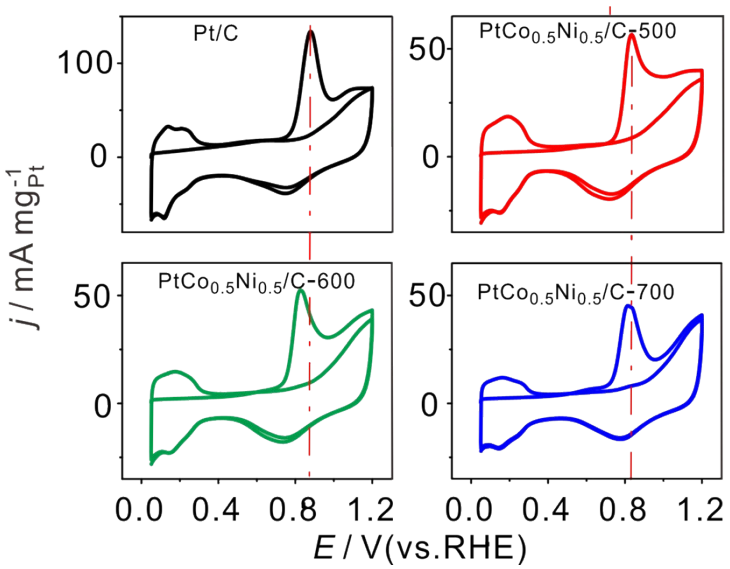

Figure S11. CO stripping voltammograms curves of $PtCo_{0.5}Ni_{0.5}/C$ annealing at different temperatures for 2 h and Pt/C catalysts in 0.5 M H_2SO_4 solution at room temperature and at a scan rate of 50 mV s^{-1}.

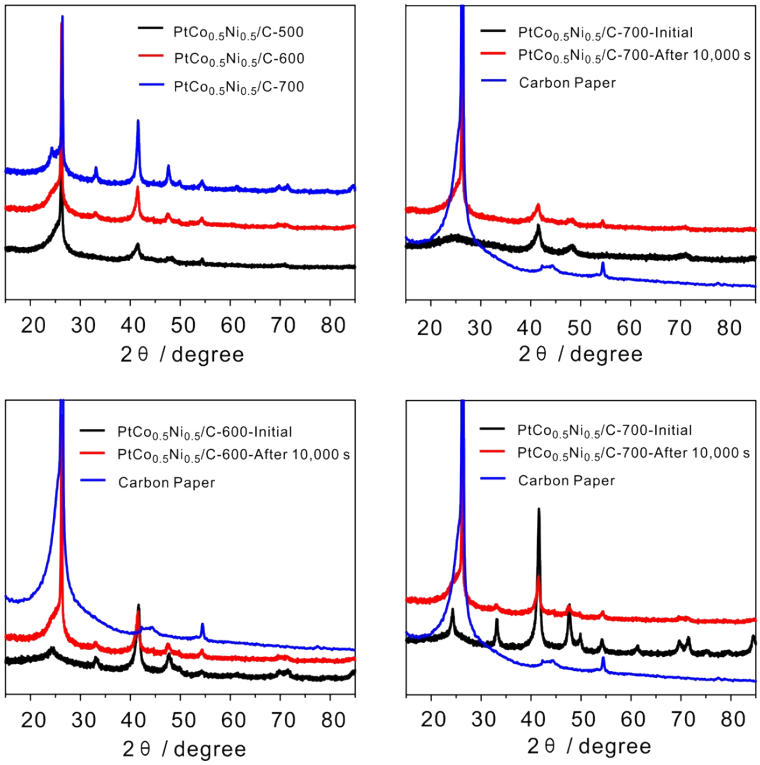

Figure S12. XRD patterns for $PtCo_{0.5}Ni_{0.5}/C$ annealing at different temperatures for 2 h before and after CA measurements.

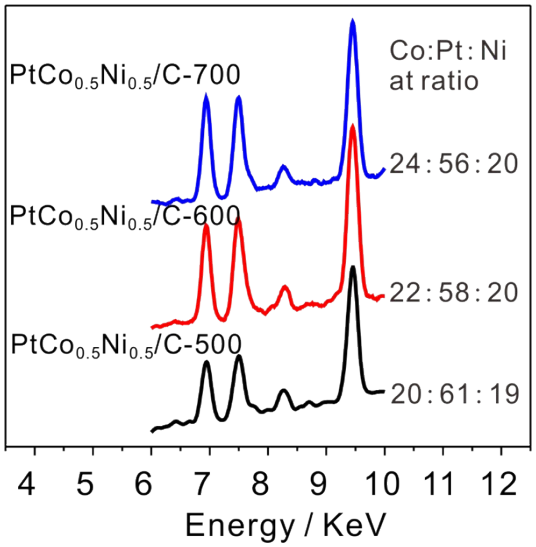

Figure S13. XRF patterns of $PtCo_{0.5}Ni_{0.5}$/C after CA measurements.

1. Y. Wen, F. Ren, T. Bai, H. Xu, Y. Du, *Colloid Surf. A-Physicochem. Eng. Asp.*, 2018, **537**, 418-424.
2. B. Habibi, N. Delnavaz, *RSC Adv.*, 2015, **5**, 73639-73650.
3. B. Habibi, N. Delnavaz, *RSC Adv.*, 2012, **2**, 1609-1617.
4. B. Habibi, N. Delnavaz. *Int. J. Hydrogen Energy*, 2011, **36**, 9581-9590.
5. B. Habibi, S. Mohammadyari, *J Taiwan Inst Chem Eng.* 2016, **58**, 245-251.
6. X. Lu, F. Luo, H. Song, S. Liao, H. Li, *J. Power Sources*, 2014, **246**, 659-666.
7. D. N. Oko, J. Zhang, S. Garbarino, M. Chaker, D. Ma, A. C. Tavares, D. Guay, *J. Power Sources*, 2014, **248**, 273-282.
8. S. Zhang, S. Guo, H. Zhu, D. Su, S. Sun, *J. Am. Chem. Soc*., 2012, **134**, 5060-5063.
9. Z. Yao, M. Zhu, F. Jiang, Y. Du, C. Wang, P. Yang. J. Mater. Chem., 2012, **22**, 13707-13713.
10. Z. Li, M. Li, M. Han, X. Wu, Y. Guo, J. Zeng, Y. Li, S. Liao, *J. Power Sources*, 2015, **278**, 332-339.
11. C. Zhai, M. Zhu, D. Bin, F. Ren, C. Wang, P. Yang, Y. Du, *J. Power Sources*, 2015, **275**, 483-488.
12. X. Zhang, B. Zhang, D. Liu, J. Qiao. *Electrochim. Acta*, 2015, 177, 93-99.
13. C. Xu, Q. Hao, H. Duan, *J. Mater. Chem. A*, 2014, **2**, 8875-8880.
14. J. Zhu, X. Zheng, J. Wang, Z. Wu, L. Han, R. Lin, H. L. Xin, D. Wang, *J.Mater. Chem. A*, 2015, **3**, 22129-22135.